GEOPHYSICAL RESEARCH LETTERS, VOL. 26, NO.5, PAGES 549-552, MARCH 1, 1999

A map of topography on the 410-km discontinuity from PP precursors

Megan P. Flanagan and Peter M. Shearer

Cecil H. and Ida M. Green Institute of Geophysics and Planetary Physics, Scripps Institution of Oceanography, University of California, San Diego, La Jolla

Abstract.
We derive a new map of global topography on the 410-km discontinuity from observations of precursors to PP obtained by stacking almost 25,000 long-period seismograms. The inferred '410' topography exhibits average peak-to-peak amplitude of about 30 km, has a strong degree-one component, and is highly correlated with previous results obtained from SS precursors [*Flanagan and Shearer*, 1998]. Spatial variations in '410' topography appear unrelated to ocean-continent differences, suggesting that continental roots are not a significant factor in observed global temperature variations at 410 km depth.

Introduction

Global maps of the large-scale topography on the 410- and 660-km discontinuities can be produced using observations of long-period precursors to SS that result from underside reflections off these interfaces [e.g., *Shearer*, 1991, 1993; *Gossler and Kind*, 1996; *Gu and Dziewonski*, 1998; *Flanagan and Shearer*, 1998]. These maps can be used to infer temperature variations at certain depths (using laboratory results for the Clapeyron slopes for the appropriate phase changes in olivine) with much greater vertical resolution than is currently possible using mantle tomography. It is well known that seismic velocities within the uppermost ~200 km of the mantle are faster beneath continents than oceans, but the full depth extent of these fast continental roots is not well constrained. Most mantle tomography models [e.g., *Masters et al.*, 1996] show a significant difference between oceans and continents at a depth of 400 km, but the limited vertical resolution of the tomographic inversions admits the possibility that this is an inversion artifact caused by leakage from velocity anomalies at shallower depths.

Thus, observed topography on the 410-km discontinuity derived from SS precursors provides an important test of the depth extent of ocean-continent differences in temperature profiles. Results to date, however, have yielded conflicting conclusions. *Gossler and Kind* [1996] mapped transition zone thickness (the difference between the depths to the 410- and 660-km discontinuities) and found evidence for ocean-continent differences, suggesting that continental roots extend at least to 400 km. *Gu and Dziewonski* [1998] identified an ocean-continent signal in their map of '410' topography, again supporting the deep root hypothesis. However, maps of '410' topography produced by *Shearer* [1993] and *Flanagan and Shearer* [1998] show no significant variation in average depths between oceans and continents. In addition, *Li et al.* [1998] recently used P-to-S converted phases from the MOMA array across eastern North America to show that the 410-km discontinuity is not significantly perturbed in the region beneath the eastern boundary of the continental root.

Here, we derive a new map of topography on the 410-km discontinuity using observations of long-period precursors to PP. Our results agree closely with our previous topography models based on SS precursors [*Flanagan and Shearer*, 1998, henceforth termed $FS98$] but were derived from completely different data. Our '410' topography model is dominantly degree-one and does not appear related to ocean-continent differences.

Stacking PP Precursors

Our approach closely follows that used by $FS98$ to analyze SS precursors. We use long-period, vertical-component seismograms recorded by the GDSN (1976–1997), IRIS-IDA (1988–1997), and GEOSCOPE (1988–1997) networks, selecting records with $m_b > 5.5$, focal depth < 100 km, and range 80° to 180°. To enhance the visibility of the discontinuity reflections, we align the seismograms on the maximum amplitude of the PP arrival, and stack the data in bins of constant source-receiver range. Figure 1 is a time versus range image derived from all 24,667 waveforms (A, B, and C quality) stacked in 0.5° range bins. Plotted above are theoretical travel time curves for several phases in this time window calculated from iasp91 [*Kennett*, 1991]. The stacking process assigns greater weight to those records with low noise levels as measured in a window 120 to 40 s prior to PP.

The underside reflection $P410P$ is clearly apparent, arriving about 84 s before PP in the range 100° to 142°, although it is obscured by the PKP arrival between 118° and 126°. At ranges beyond 142°, $P410P$ is hidden by the topside discontinuity reflections following

Paper number 1999GL900036.
0094-8276/99/1999GL900036$05.00

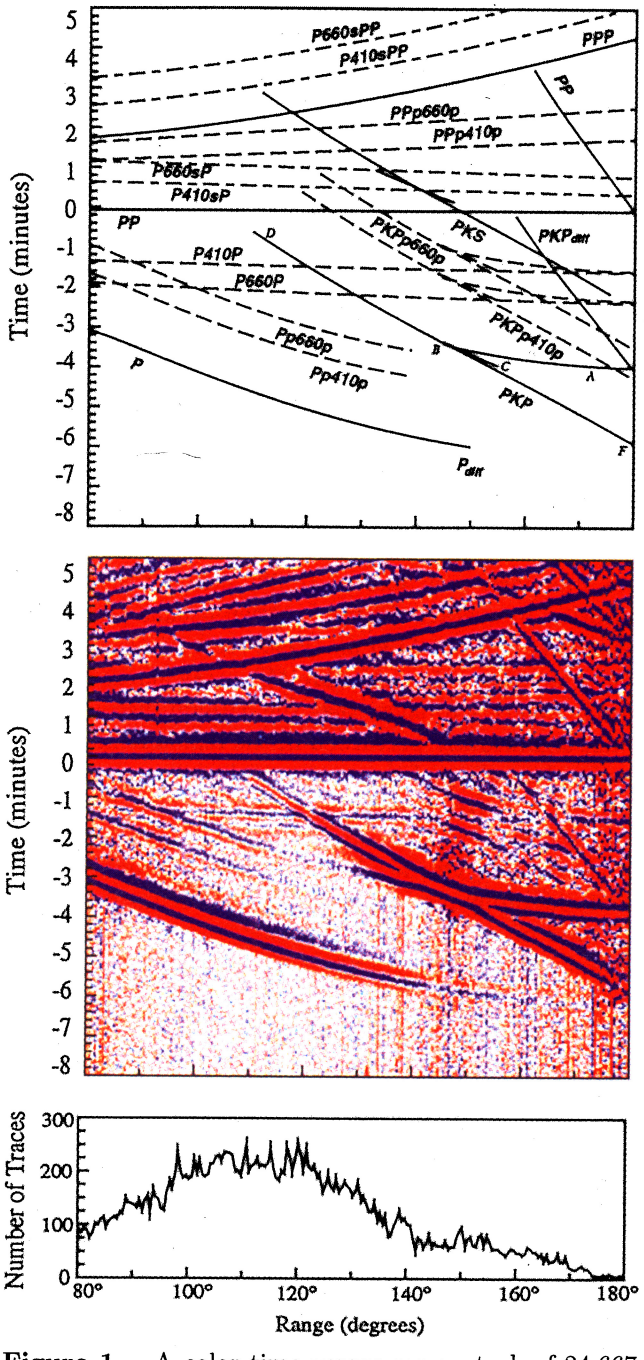

Figure 1. A color time versus range stack of 24,667 long-period seismograms showing PP and its precursors. PP is normalized to zero time and unit amplitude; positive amplitudes are blue and negative are red, and the scale is $\pm 5\%$ of the PP amplitude. The upper plot shows travel-time curves for the primary phases (solid lines) and transition zone discontinuity phases (dashed); the lower plot shows the range distribution of the data.

$PKP(BC)$. A weak $P520P$ phase is observed between 110° and 125° while no $P660P$ phase is observed at any epicentral range. The absence of $P660P$ in stacks of long-period PP [see also *Shearer*, 1991] corroborates the results of *Estabrook and Kind* [1996] and supports their conclusion that the underside P reflection at 120° range is much smaller than predicted by most P velocity models.

Our interest in this paper, however, is in $P410P$, the most visible of the long-period PP precursors. To investigate variations in depth to the 410-km discontinuity, we use two subsets of the data shown in Figure 1 which lie between 100° to 118° and 126° to 142°. The distribution of bounce point locations are plotted in Figure 2, showing the particularly dense coverage in much of the Pacific and Indian Oceans. Despite the restricted range intervals for $P410P$ observations, the number of data and the spatial coverage are comparable to that obtained in recent global SS precursor studies [e.g., *Gu and Dziewonski*, 1998; $FS98$].

Cap-Averaging Method

To explore global variations in depths to the 410-km discontinuity, we divide the data by their bounce point location into 416 caps of 10° radius. Records within each cap are then stacked along the theoretical travel-time curve for $P410P$ to a reference range of 138° (PP is stacked separately along its travel time curve), with greater weight assigned to records with low noise levels. We identify and time the peak positions of the $P410P$ precursors on the individual stacks and estimate standard errors using the bootstrap resampling method of $FS98$.

Next, the PP–$P410P$ times and their associated standard errors are converted to discontinuity depths using isotropic PREM at 25 s period [*Dziewonski and Anderson*, 1981]. Apparent '410' discountinuity depths are shown in Figure 3a; depths are measured for 281 caps and plotted as perturbations about their global mean. Crosses indicate deeper regions, and diamonds indicate shallower regions with the size of the symbol scaling with the depth variation. These raw depth estimates exhibit peak-to-peak topography of roughly 40 km, with large-scale coherent patterns of elevated and depressed regions.

Because these depth estimates are likely to be biased by surface topography, crustal structure, and upper-mantle P velocity variations, we apply timing corrections to the PP–$P410P$ times to account for these

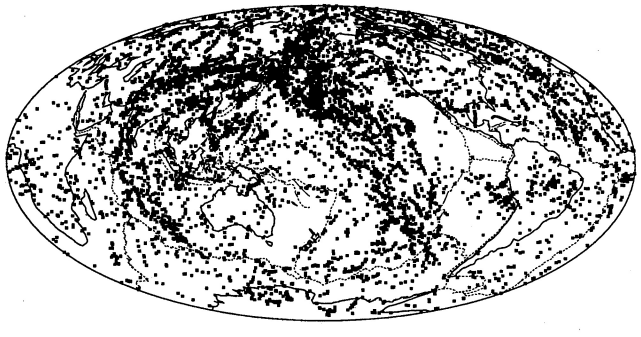

Figure 2. Global distribution of the PP bounce points from the 10,466 seismograms used to map 410-km discontinuity topography. These data are from epicentral ranges 100° to 118° and 126° to 142°, the intervals in which $P410P$ is most visible.

effects. Our corrections are computed from the regionalized global crustal model $CRUST5.1$ [*Mooney et al.*, 1997] and the P-wave mantle tomography model $P16B30$ [*Bolton*, 1996]. In addition, we apply a correction to account for absolute P travel times through the upper mantle (as the adjustment of PREM to the crustal model produces a baseline shift in travel times, see $FS98$). The corrected depth estimates are plotted in Figure 3b; notice the corrected '410' depths are slightly deeper than the raw depths. The average corrected depth of 419 km is in good agreement with the 418 km estimate obtained from SS precursors by $FS98$. The variance in the corrected depths is reduced compared to the raw depths, but the overall pattern of highs and lows is largely unchanged.

410-km Discontinuity Topography

The spatial coverage shown by the caps in Figure 3 is sufficient to permit the construction of smooth maps of the global '410' topography. We use the method of spherical splines to fit the individual cap values (including their standard errors) and then compute the equivalent spherical harmonic expansion of the splined field up to degree 12 (as in $FS98$). The resulting smooth map is shown in Figure 4 together with the SS precursor model of $FS98$. The peak-to-peak topography in these models is 27 km for the PP model and 22 km for the SS model (this difference is probably not significant, as the peak-to-peak amplitude in the models is a strong function of the amount of smoothing applied in the fit). Note the strong correlation between the models: each has a strong degree-one pattern with a broad depression beneath the Pacific Ocean and South America, and elevations beneath the Indian Ocean as well as parts of Antarctica and Africa. Depth and differential time values for the individual caps and the spherical harmonic coefficients for the smooth PP model are available from the authors via e-mail or ftp at mahi.ucsd.edu in the /pub/TOPOPP directory.

Although the models disagree in some of their details (mainly in areas of sparse data coverage), the agreement between their dominant features supports the validity of using PP and SS precursor observations to map upper-mantle discontinuity topography. These models were obtained using different data sets and different corrections for upper-mantle structure. The 410-km discontinuity topography, as mapped by either the PP or SS precursors, does not appear related to surface tectonic features. Significant elevations of the '410' are not observed near subduction zones; clear '410' depth anomalies are not seen near spreading ridges, consistent with the absent of a transition zone temperature anomaly for the East Pacific Rise noted by *Lee and Grand* [1996].

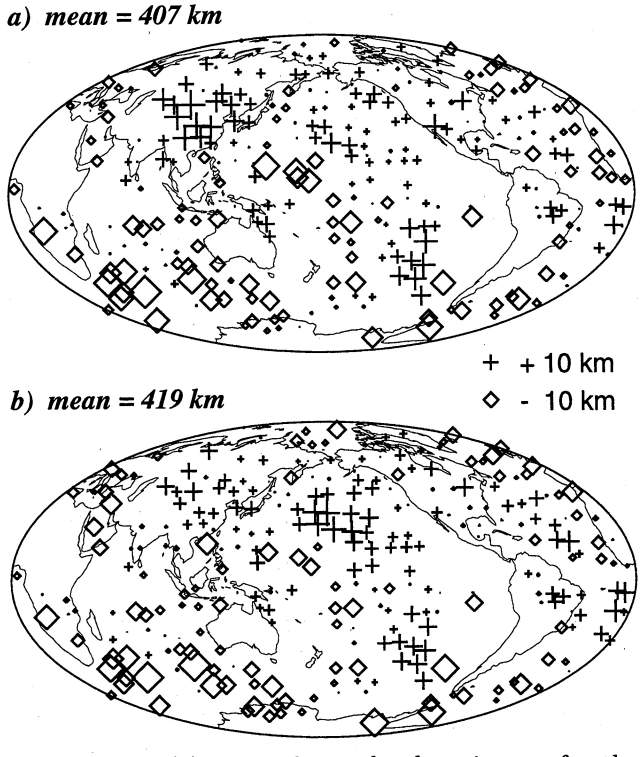

Figure 3. (a) Map of raw depth estimates for the 410-km discontinuity plotted at the centroid location of bounce points for each cap. Crosses indicate depressions and diamonds indicate elevations relative to the mean discontinuity depth. Depth estimates are plotted only if the cap contains 10 or more seismograms and the standard error is less than 15 km. (b) Map of the corrected depth estimates, computed after applying corrections for surface topography, crustal thickness, and upper mantle P-wave velocity structure.

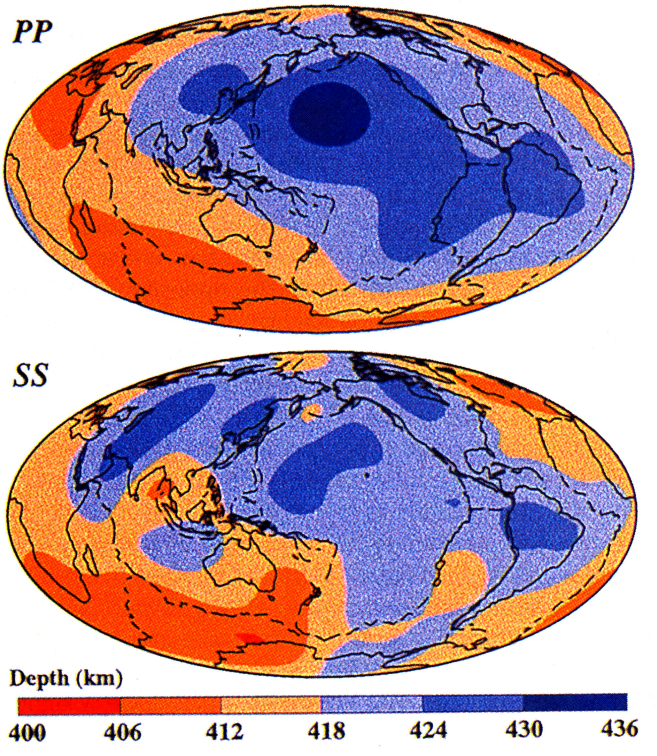

Figure 4. Smooth maps of '410' topography derived from precursors to PP (this study) and SS (FS98). These surfaces are produced using the method of spherical splines applied to the cap averages shown in Figure 4.

This suggests that any thermal anomalies associated with either subduction zones or spreading ridges must be too narrow to be resolved with these long-period data (which have Fresnel zones about 10° across).

The 410-km discontinuity topography also does not appear clearly related to ocean-continent differences, as was suggested by the *SS* precursor study of *Gu and Dziewonski* [1998] in which '410' depths under continents were about 5 km shallower than under oceans. If anything, our results show the opposite, with several continents appearing slightly depressed compared to the global average; however, this difference is insignificant compared to the much larger depth variations observed else, such as the 20 to 30 km difference in '410' depths between the north Pacific and Indian oceans. Our topography models are only weakly correlated with the '410' topography model of *Gu and Dziewonski*; the much closer agreement between our *PP* and *SS* models is additional evidence to support our conclusion that ocean-continent differences are an insignificant factor in '410' topography. Most *P* and *S* tomography models [e.g., *Masters et al.*, 1996; *Bolton*, 1996] show velocity anomalies near 400 km depth which have a significant ocean-continent signal (i.e., fast beneath continent and slow beneath oceans). The absence of such a signal in our observed '410' topography has two likely explanations: (1) The tomography results are biased near 400 km by leakage of shallow velocity anomalies to greater depths, or (2) The interpretation of both discontinuity topography and mantle velocity anomalies near 400 km as resulting from temperature differences is too simplistic. If the latter explanation is correct, then it is likely that compositional variations in mantle properties are important near 400 km depth.

Acknowledgments. K. Dueker and two anonymous reviewers provided helpful comments. This research was supported by NSF grant EAR96-14350. M.P.F. received support from an NSF Postdoctoral Fellowship and the Cecil H. and Ida M. Green Foundation.

References

Bolton, H., *Long period travel times and the structure of the mantle*, Ph.D. thesis, University of California, San Diego, La Jolla, CA, 204 pp., 1996.

Dziewonski, A.M., and D.L. Anderson, Preliminary reference Earth model, *Phys. Earth Planet. Inter.*, *25*, 297–356, 1981.

Estabrook, C.H., and R. Kind, The nature of the 660-km upper-mantle seismic discontinuity from precursors to the *PP* phase, *Science*, *274*, 1179–1182, 1996.

Gossler, J. and R. Kind, Seismic evidence for very deep roots of continents, *Earth Planet. Sci. Lett.*, *138*, 1–13, 1996.

Gu, Y., A.M. Dziewonski and C.B. Agee, Global de-correlation of the topography of transition zone discontinuities, *Earth Planet. Sci. Lett.*, *157*, 57–67, 1998.

Flanagan, M.P. and P.M. Shearer, Global mapping of topography on transition zone velocity discontinuities by stacking *SS* precursors, *J. Geophys. Res.*, *103*, 2673–2692, 1998.

Kennett, B.L.N., editor, *IASPEI 1991 Seismological Tables*, Research School of Earth Sciences, Australian National University, Canberra, 1991.

Lee, D.-K., and S.P. Grand, Depth of the upper mantle discontinuities beneath the East Pacific Rise, *Geophys. Res. Lett.*, *23*, 3369–3372, 1996.

Li, A., K.M. Fischer, M.E. Wysession and T.J. Clarke, Mantle discontinuities and temperature under the North American continental keel, *Nature*, *395*, 160–163, 1998.

Masters, G., S. Johnson, G. Laske and H. Bolton, A shear-velocity model of the mantle, *Philos. Trans. R. Soc. London*, *354*, 1385–1411, 1996.

Mooney, W.D., G. Laske and T.G. Masters, CRUST 5.1: A global crustal model at 5° × 5°, *J. Geophys. Res.*, *103*, 727–747, 1998.

Shearer, P.M., Constraints on upper mantle discontinuities from observations of long-period reflected and converted phases, *J. Geophys. Res.*, *96*, 18,147–18,182, 1991.

Shearer, P.M., Global mapping of upper mantle reflectors from long-period *SS* precursors, *Geophys. J. Int.*, *115*, 878–904, 1993.

M.P. Flanagan and P.M. Shearer, IGPP 0225, Scripps Institution of Oceanography, University of California, San Diego, La Jolla, CA, 92093-0225 (megan@mahi.ucsd.edu, pshearer@ucsd.edu).

(Received November 3, 1998; revised December 21, 1998; accepted January 6, 1999.)